Investigation of Power Coefficient Behaviors of the Parabolic Wind Rotor Due to its Variable Geometry Parameters

Hashem Abusannuga *‡, Mehmet Özkaymak **

*Energy Systems Engineering, Faculty of Technology, Karabuk University, Turkey

** Energy Systems Engineering, Faculty of Technology, Karabuk University, Turkey

(hashem_ebrahim@yshoo.com, mozkaymak@karabuk.edu.tr,)

‡ Corresponding Author; Hashem Abusannuga, Energy Systems Engineering, Faculty of Technology, Karabuk University, Tel: +90 5432219323, hashem_ebrahim@yahoo.com

Received: 30.12.2020 Accepted:31.01.2020

Abstract- This paper provides explanations and analysis of how the power coefficient (Cp) of the Parabolic wind rotor has been affected by changing its geometrical design parameters. The results were presented in the form of (Cp) curves as a function of tip speed ratio (λ_0). The aerodynamic mathematical mode called "multi-streamtube" was implemented. To determine the Cp(λ_0) of the Parabolic rotor, regardless of its engineering shape, a computer program has been prepared by using Microsoft Visual Basic. The geometrical design parameters covered in this study are rotor blades number (N), rotor height (h) or (2H), rotor diameter (2R) and chord line (C). Whereas, through these parameters a total of 57 configurations were utilized and adopted. Thus, this number of different designs was sufficient to identify the performance behaviors of the Parabolic wind rotor. Accordingly, the results indicated that increasing rotor height to diameter ratio (H/R) leads to a decrease in Cp over low tip speed ratio range for all values of solidity,σ, (NC/R) investigated. However, higher values of (H/R) result in a raise in Cp over high tip speed ratio range for values of (NC/R) less than 0.2 approximately. Thus, it seems that higher (H/R) values constitute an advantage for fast rotating rotors (low (NC/R) and high tip speed ratio).

Keywords VAWT, Parabolic wind rotor, Aerodynamic performance.

1. Introduction

Wind energy is one of the most famous and widely used renewable energies today [1]. A wind turbine is a machine that a human invented to diversion the kinetic energy in the wind into electrical energy. Wind turbines are divided into two main categories, where they are classified according to the direction of the axis of rotation, the first and most used class is "Horizontal-Axis Wind Turbine" or "HAWT In this type, the air fan rotates so that the rotating axis is parallel to the Earth's surface, and that is the reason for its name. Secondly, what is known as the " Vertical Axis Wind Turbine", whose axis of rotation is perpendicular to the surface of the earth and hence it called "VAWT". Horizontal axis turbines they are widely used and have a higher efficiency than vertical axis turbines, but in contrast to vertical axis turbines, horizontal axis type has less negative impact on the environment and has attracted researchers due to its advantages. The most important of these advantages are: No dependence on wind direction, low maintenance cost, low noise. [2-7].

Wind turbines, either horizontal or vertical, consist of a group of basic parts which are wind rotor, the gearbox, the electrical generator, control system, and the tower. The wind rotor is one of the most important parts because it is responsible for converting the kinetic energy in the wind into mechanical energy that is transferred to the gearbox. The gearbox transmits this shaft power to the electrical generator in addition to raising up the shaft rotational speed to a predetermined value. There are two types of systems in which wind turbines operate, which is the system isolated from the electrical network "stand alone", and the other is a system connected to the electrical network "grid connected".[8]

Nowadays there are many different designs for Vertical axis wind systems, and they compete in terms of performance, whether in terms of the amount of energy extracted from the wind or aerodynamic stability. Some important designs for these systems are Straight-Blade VAWT [9][28], Troposkien

VAWT [10] [11], Hlical VAWT [12], Counter Rotating [13] and Vortex Bladeless Wind Turbine [14].

The performance of the wind rotor is described in a "nondimensional" parameters, which makes that performance suitable for use regardless of the actual rotor size, as long as the "engineering similarity" is maintained. For this reason, the performance of the wind rotor is usually presented in the form of curves represented by the power coefficients CP, as a function of tip speed ratio λ_0, which is also an "nondimensional" parameter.

As the title of this paper indicates, the present study seeks to investigate the effects on power coefficient of Parabolic vertical wind rotor by change some of the main geometrical design parameters. There is no doubt that knowing the effect of the variables of the engineering shape contributes to knowing the behaviour of the rotor and checking it, and this would provide us with the best design of the rotor in terms of the maximum power coefficient and the corresponding tip speed ratio in addition to the amount of energy extracted from the wind. In this regard, the following engineering parameters were studied **:** rotor blades number (N), blade chord to rotor radius ratio (C/R), rotor height to diameter ratio (H/R), and rotor solidity (NC/R).

2. Rotor Configurations Studied

In order to keep track of these configurations a labeling scheme has been adopted. The label starts with two or three letters which refer to the parameter being investigated, followed by three digits, which when divided by 100 they give the actual value of that parameter. Following these three digits there are the letters "HR" which stand for the rotor height to diameter ratio at which the parameter was varied. The actual value of (H/R) is given by the last three digits divided by 100.

The letter groups, BN, CR, NCR, and HR has been assigned respectively to the following design parameters: "blades number", "chord to radius ratio", "solidity" and "height to radius ratio". To explain further what the labels indicate, the configuration label "CR012HR067" is explained. Here "CR" indicates that the parameter being investigated is chord to radius ratio while the actual value is (C/R) = 0.12. Moreover, (C/R) is being investigated at a value of (H/R) = 0.67. Table (1) presents geometrical details of all the rotor configurations employed in this work.

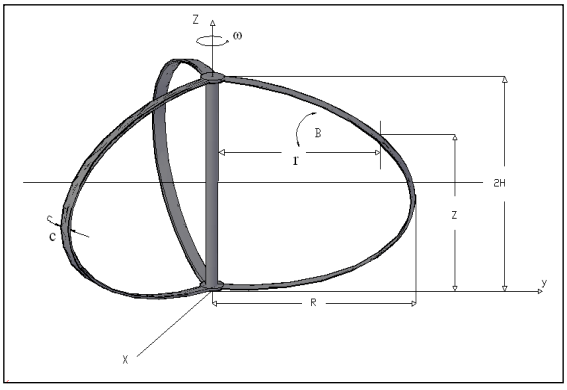

Fig. 1. Ggeometrical parameters of parabolic Darrieus rotor.

3. Mathematical Models for Design and Performance Analysis of VAWT

According to published reports and studies there are a number of analytical or theoretical methods that can be used to study and determine the performance of VAWT wind rotor [26] [27]. Most of these methods aim to determine the field of air velocity during the rotor which is quite different from the regular distribution of the wind speed coming on it. Determination of the velocity range during the rotor leads to the determination of the aerodynamic forces that affect the blades and thus enables the determination of the torque and power values it generates.

Templin [15] used a technique known as "Single Streamtube" where it replaced the rotor with what is known as an "actuator disk". Within this method, the velocity field during the rotor is determined by the equations of two axial forces, one of which is derived from the calculation of the kinetic forces of the air in the axial direction and the other is derived using the general theory of axial momentum theory.

At the same time Lissaman & Wilson [16] and then Strickland [17] and Read & Sharpe [18] developed the Templin method and considered that there were a number of "streamtubes" permeating the rotor, making the value of air velocity variable with the change of location through "actuator disk". To take into account the speed difference between the rotor blades coming in the direction of the wind and those arranged for it, Lapin [19] suggested the use of two drives respectively. Paraschivoiu [20] exploited Lapin 's work and advanced the work style currently known as "Double - Multiple Streamtube".

Fanucci & Walters [21], Holme [22], and Strickland [23] have developed a completely different approach than the aforementioned methods called "Vortex method". In this procedure, the blade of rotor is superseded by a system of vortices as applied in the aeronautics of the wing of the aircraft and then the induced velocity of the system is calculated at different points in the rotor level. Adding the wind speed coming on to the rotor can then determine the speed field across the entire rotor.

Due to some similarities between the Darius rotor blade pattern of straight blades and some of the so-called "turbomachinery" blades, Hirsch & Mandal [24] introduced a method called "Cascade Model". The method of determining the range of velocity across the rotor is based on a relationship between the velocity of the air behind the rotor and the incoming wind speed using the Bernoulli equation, as well as the use of a theoretical-experimental formula that links the induced velocity through the rotor to the speed behind it.

3.1. Multiple Streamtube Model

In this study, "Multiple-streamtube" method has been used. Below is a brief description of this method according to what Strickland has published [25]. As shown in Figure (2), the rotor is replaced by what is known as an "actuator disc" or rather an actuator cylinder. This disk is punctuated by a number of what is known as "streamtube". It is an imaginary tube-shaped stream whose surface consists of flowlines or

what is known as "streamlines" and therefore the velocity vector is tangential at any point on its surface. The speed of the air through the disk changes from one streamtube to another, just as the speed of the air during any streamtube changes from its value of free stream velocity "V_1" away in front of the rotor to its value of air velocity in rotor plane "V" in the disk level and finally to its value of wake velocity "V_2" far behind the rotor. And this constant change in speed occurs as a result of the rotor extracting part of the movement energy that lies in the wind blowing on it.

The power P is given by:

$$P = \frac{\rho N C}{2\pi} \int_0^H \int_0^\pi W^2 r \frac{\omega C_t}{\sin\beta} d\theta dz \quad (1)$$

Tip speed ratio is defined as follows:

$$\lambda_\circ = \frac{\omega R}{V_1} \quad (2)$$

The power coefficient is:

$$C_P = \frac{P}{{}^1/_2 \rho V_1^3 A} \quad (3)$$

Also, from equation (1) and (2) Cp become:

$$C_p = \frac{NC}{\pi A} \int_0^H \int_0^\pi \left(\frac{W}{V_1}\right)^2 \lambda_0 \frac{r}{R} \frac{C_t}{\sin\beta} d\theta dz \quad (4)$$

ω ≡ angular velocity

ρ ≡ air density

P ≡ power

W ≡ resultant velocity

A ≡ rotor swept area

$C_t \equiv C_l \sin\alpha - C_d \cos\alpha$

C_l ≡ lift coefficient

C_d ≡ drag coefficient

θ ≡ azimuth angel

β ≡ blade inclination angle

z ≡ blade element hight

r ≡ radius at a blade element

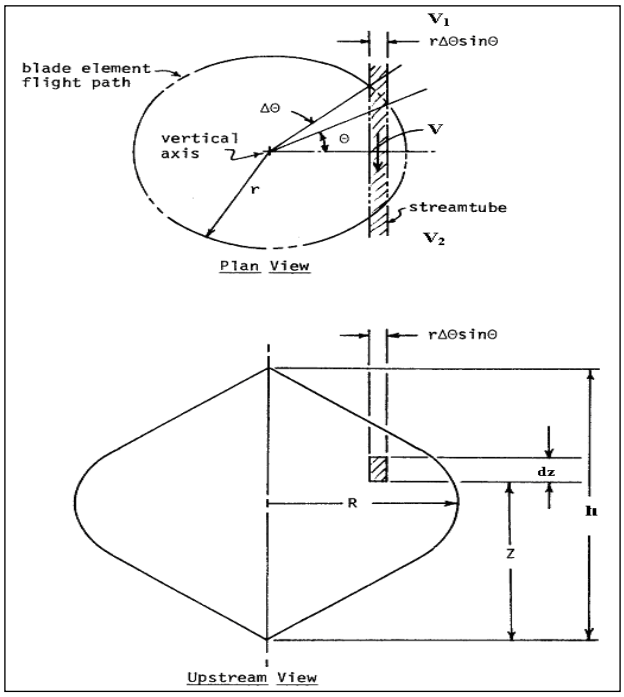

Fig. 2. Geometrical aspects of "Multiple-Streamtube Model" and relevant velocities.

4. Discussions and Results

4.1. Number of Blades Influence, N. [Group. I]

In order to study the effect of changing the number of rotor blades, configurations listed under group I in table (1) were employed in which H/R, C/R, and airfoil data were all kept constant while N was varied from 1 to 5. Fig (3) depicts the variation of power coefficient, Cp, as a function of tip speed ratio, λ_0 for a value of rotor height to diameter ratio of 0.67. It can be seen that as N increases the maximum value of power coefficient, C_{PM}, increases at first but then it slightly decreases.

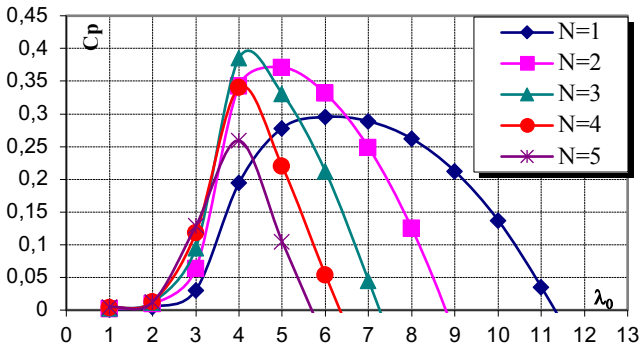

Fig. 3. The influence of (N) on the Cp(λ_0) Curves with (C/R) = 0.09 and (H/R) = 0.67.

It is also noted that the value of λ_0 at which C_{PM} occurs shifts towards lower values as N increases. This in turn indicates that as N increases the rotor would rotate at relatively lower speeds which necessitate relatively larger gear-up ratios. The increase in N also makes the Cp(λ_0) curve "peaky", which leads to a narrower range of λ_0 over which the rotor

operates more efficiently. Over the lower range of λ_0, an increase in N leads to an increase in Cp except for N larger than 4. The reverse is true over the high λ_0-range. However, as the rotor height to diameter ratio (H/R) increases, some modifications to the behavior of the $Cp(\lambda_0)$ curves occur as N increases. This is clearly seen in figures (4) and (5) in which values of height to diameter ratios are respectively 1.0 and 1.5. For instance, the value of Cp_m decreases for values of N exceeding 3, 2, and 2 for the cases of height to diameter ratios of 0.67, 1.0, and 1.5 respectively. Another example is the increase (or decrease) of Cp over the low λ_0-range with increasing N for the various height to diameter ratios.

At low rotational speeds, the local blade-section angle of attack is relatively high. The flow regime is thus dominated by flow separation which generally leads to lower values of C_l to C_d ratio. Under such circumstances, an increase in N simply means an increase in total blade surface area which in turn enables the rotor to produce relatively more torque and consequently more power. However, at high rotational speeds, an increase in N or equivalently an increase in rotor total blade area increases what might be termed "flow blockage" whereby a portion of the oncoming wind is forced to flow around the rotor instead of flowing through it. This by-pass of air around the rotor would definitely reduce the amount of available wind power.

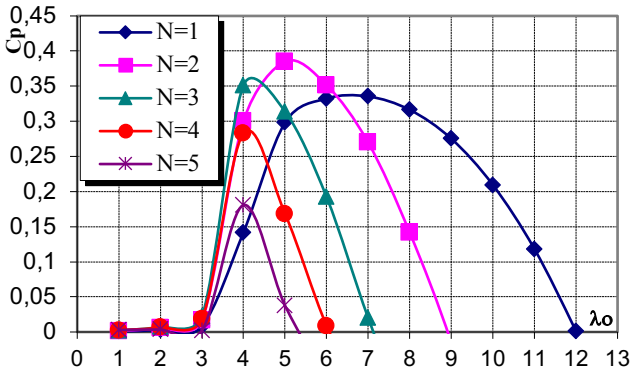

Fig. 4. The influence of (N) on the $Cp(\lambda_0)$ Curves with (C/R) = 0.09 and (H/R) = 1.

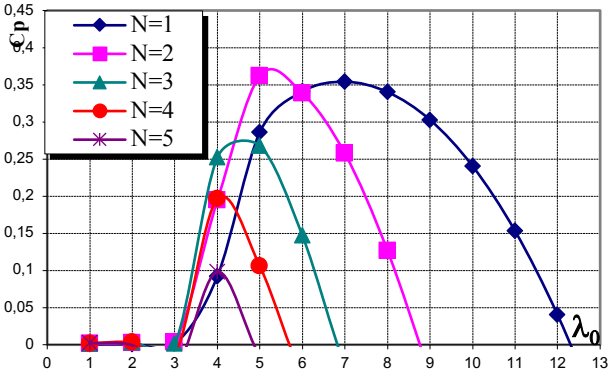

Fig. 5. The influence of (N) on the $Cp(\lambda_0)$ Curves with (C/R) = 0.09 and (H/R) = 1.5.

Table 1. Geometrical details of the 57 rotor configurations employed in the present study.

Configuration	H (m)	R (m)	C (m)	N (-)	H/R (-)	C/R (-)	NC/R (-)
Group. I	Effect of Number of Blades (N)						
BN100HR067	0.67	1	0.09	1	0.67	0.09	0.09
BN200HR067	0.67	1	0.09	2	0.67	0.09	0.18
BN300HR067	0.67	1	0.09	3	0.67	0.09	0.27
BN400HR067	0.67	1	0.09	4	0.67	0.09	0.36
BN500HR067	0.67	1	0.09	5	0.67	0.09	0.45
BN100HR100	1	1	0.09	1	1	0.09	0.09
BN200HR100	1	1	0.09	2	1	0.09	0.18
BN300HR100	1	1	0.09	3	1	0.09	0.27
BN400HR100	1	1	0.09	4	1	0.09	0.36
BN500HR100	1	1	0.09	5	1	0.09	0.45
BN100HR150	1.5	1	0.09	1	1.5	0.09	0.09
BN200HR150	1.5	1	0.09	2	1.5	0.09	0.18
BN300HR150	1.5	1	0.09	3	1.5	0.09	0.27
BN400HR150	1.5	1	0.09	4	1.5	0.09	0.36
BN500HR150	1.5	1	0.09	5	1.5	0.09	0.45
Group. II	Effect of Chord to Radius Ratio (C/R)						
CR003HR067	0.67	1	0.03	3	0.67	0.03	0.09
CR006HR067	0.67	1	0.06	3	0.67	0.06	0.18
CR009HR067	0.67	1	0.09	3	0.67	0.09	0.27
CR012HR067	0.67	1	0.12	3	0.67	0.12	0.36

CR015HR067	0.67	1	0.15	3	0.67	0.15	0.45
CR003HR100	1	1	0.03	3	1	0.03	0.09
CR006HR100	1	1	0.06	3	1	0.06	0.18
CR009HR100	1	1	0.09	3	1	0.09	0.27
CR012HR100	1	1	0.12	3	1	0.12	0.36
CR015HR100	1	1	0.15	3	1	0.15	0.45
CR003HR150	1.5	1	0.03	3	1.5	0.03	0.09
CR006HR150	1.5	1	0.06	3	1.5	0.06	0.18
CR009HR150	1.5	1	0.09	3	1.5	0.09	0.27
CR012HR150	1.5	1	0.12	3	1.5	0.12	0.36
CR015HR150	1.5	1	0.15	3	1.5	0.15	0.45
Group. III	Effect of Solidity, σ, (NC/R)						
NCR09HR067	0.67	1	0.09	1	0.67	0.09	0.09
NCR18HR067	0.67	1	0.09	2	0.67	0.09	0.18
NCR27HR067	0.67	1	0.09	3	0.67	0.09	0.27
NCR36HR067	0.67	1	0.09	4	0.67	0.09	0.36
NCR45HR067	0.67	1	0.09	5	0.67	0.09	0.45
NCR09HR100	1	1	0.09	1	1	0.09	0.09
NCR18HR100	1	1	0.09	2	1	0.09	0.18
NCR27HR100	1	1	0.09	3	1	0.09	0.27
NCR36HR100	1	1	0.09	4	1	0.09	0.36
NCR45HR100	1	1	0.09	5	1	0.09	0.45
NCR09HR150	1.5	1	0.09	1	1.5	0.09	0.09
NCR18HR150	1.5	1	0.09	2	1.5	0.09	0.18
NCR27HR150	1.5	1	0.09	3	1.5	0.09	0.27
NCR36HR150	1.5	1	0.09	4	1.5	0.09	0.36
NCR45HR150	1.5	1	0.09	5	1.5	0.09	0.45
Group. IV	Effect of Height to Diameter Ratio (H/R)						
NCR09HR067	0.67	1	0.09	1	0.67	0.09	0.09
NCR09HR100	1	1	0.09	1	1	0.09	0.09
NCR09HR150	1.5	1	0.09	1	1.5	0.09	0.09
NCR18HR067	0.67	1	0.09	2	0.67	0.09	0.18
NCR18HR100	1.0	1	0.09	2	1	0.09	0.18
NCR18HR150	1.5	1	0.09	2	1.5	0.09	0.18
NCR27HR067	0.67	1	0.09	3	0.67	0.09	0.27
NCR27HR100	1	1	0.09	3	1	0.09	0.27
NCR27HR150	1.5	1	0.09	3	1.5	0.09	0.27
NCR45HR067	0.67	1	0.09	5	0.67	0.09	0.45
NCR45HR100	1	1	0.09	5	1	0.09	0.45
NCR45HR150	1.5	1	0.09	5	1.5	0.09	0.45

4.2. Chord to Radius Ratio, C/R. [Group. II]

In order to study the effects of this ratio on rotor performance, configurations CR003, CR006, CR009, CR012, and CR015 were employed. Figures (6), (7), and (8) present variation of Cp with λ_0 for different values of (C/R) at rotor height to diameter ratios of 0.67, 1.0, and 1.5. Generally speaking the value of (C/R) at a given height to diameter ratio produces similar effects (or follows the same trends) on the Cp(λ_0) curves as did the increase in N which was discussed in the previous section. The similarity between the N and (C/R) effects is due to the fact that an increase in C at constant R, for instance, simply means an increase in rotor total blade area, which is equivalent to increasing N at constant (C/R).

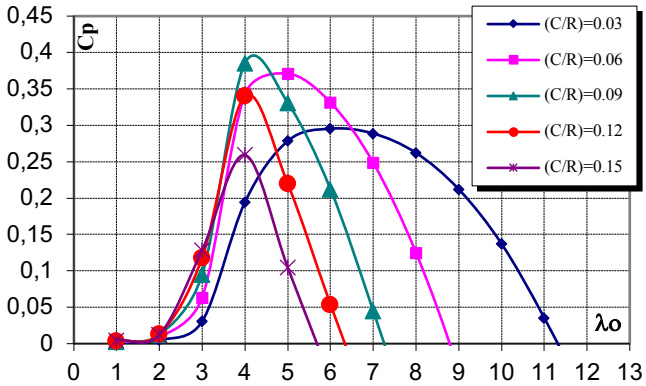

Fig. 6. The influence of (C/R) on Cp(λ_0) Curves for (N) = 3 and (H/R) = 1.

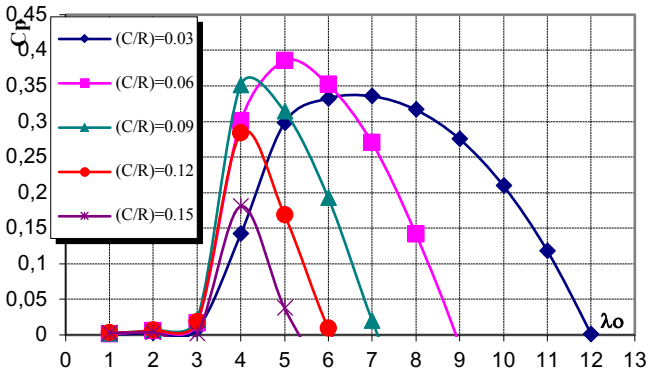

Fig. 7. The influence of (C/R) on Cp(λ_0) Curves for (N) = 3 and (H/R) = 0.67.

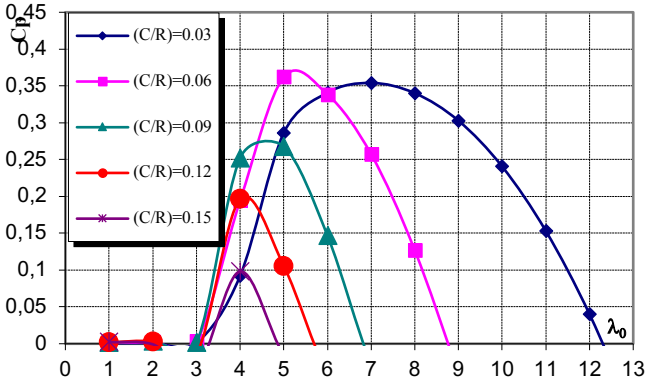

Fig. 8. The influence of (C/R) on Cp(λ_0) Curves for (N) = 3 and (H/R) = 1.5.

4.3. Solidity, σ. [Group. III]

It is common in the literature to speak of rotor solidity in terms of the ratio (NC/R). This is strictly true for straight-blade Darrieus rotor only, because the ratio of total blade area to rotor swept area, that is solidity σ, is exactly (NC/2R). This shows that σ is not function of (H/R) for straight-blade rotor. However, σ should be function of both (NC/R) and (H/R) for curved-blade rotor. To show this dependence on (H/R) consider a blade assembly consisting of N blades of constant chord C. Such blade assembly may be formed into a number of different rotor configurations with different values of swept area. Now since the total blade area of each of those different configurations is the same while the swept areas are different, the solidity is therefore different in each case.

Looking at table (1) it is noticed that the following five paris of rotor configurations have respectively values of (NC/R) equal to 0.09, 0.18, 0.27, 0.36, and 0.45 and the pairs are BN100HR100 & CR003HR100, BN200HR100 & CR006HR100, BN300HR100 & CR009HR100, BN400HR100 & CR012HR100, BN500HR100 & CR015HR100. Moreover, all of the five pairs have a value of (H/R) equal one. When the Cp(λ_0) curves for these ten configurations were plotted on the same graph, figures (9) show that the Cp(λ_0) and curves corresponding to each pair coincided exactly. This result shows that for constant value of (H/R), it is value of (NC/R) replace of the value of N or (C/R) alone which in fact determines the shape of the Cp(λ_0) curves. Such conclusion clearly shows that the blade-element method is not sensitive to the changes in the relative magnitudes of N or (C/R) as long as their product (NC/R) remains the same. Therefore, the theoretical results presented so far show that the effects of σ on Cp(λ_0) curves at constant (H/R) follow the same trends as those concerning the effects of N or (C/R) on both Cp(λ_0) curves.

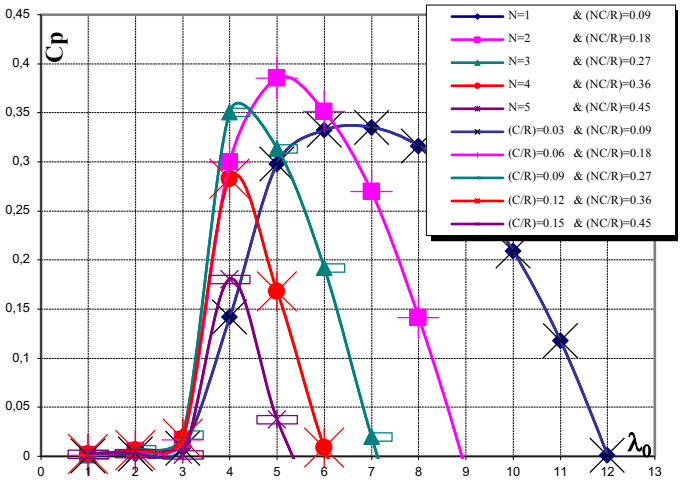

Fig. 9. varying N or (C/R) independently while keeping (NC/R) and [(H/R)=1] constants.

In practice, it is expected that varying N or (C/R) independently while keeping (NC/R) and (H/R) constants. would not lead to identical Cp(λ_0) curves. For one thing, an increase in C is bound to cause a relative increase in Cp due to the resulting increase in blade Reynolds number as will be discussed in the following section. On the other hand increasing N is expected to increase the adverse effects of the wake flow of one blade on the other.

4.4. Height to Diameter Ratio, (H/R). [Group. IV]

With the rotor height and diameter being 2H and 2R respectively, this ratio is normally expressed in terms of (H/R). In order to investigate the effects of this ratio, a value of the ratio (NC/R) equal to 0.09 was employed at first. However, upon utilizing a much larger value of (NC/R), a significant change in the trend of Cp(λ_0) curves was noticed. Therefore, a total of twelve rotor configurations were employed these configurations permitted the study of (H/R) effects at values of (NC/R) of 0.09, 0.18, 0.27, and 0.45.

Figure (10) presents Cp(λ_0) curves at constant (NC/R) of 0.09 for for three values of (H/R) which are 0.67, 1.0, and 1.5. Form this figure, it can be note that as (H/R) growing the value of Cp dwindle over low λ_0-range while it increases over the high λ_0-range. When (NC/R) is equal to 0.18, the increase in (H/R) again leads to a decrease in Cp over low λ_0-range, however, it results in slightly mixed increase-decrease behavior over high λ_0-range as can be seen in figure (11). When (NC/R) is increased further to values of 0.27 and 0.45, figures (12) and (13) show that increasing (H/R) results in a decrease in Cp over the entire λ_0-range accompanied by

a decrease in the useful λ_0-range. Negative values of Cp also appear on the left and right sides of the curves.

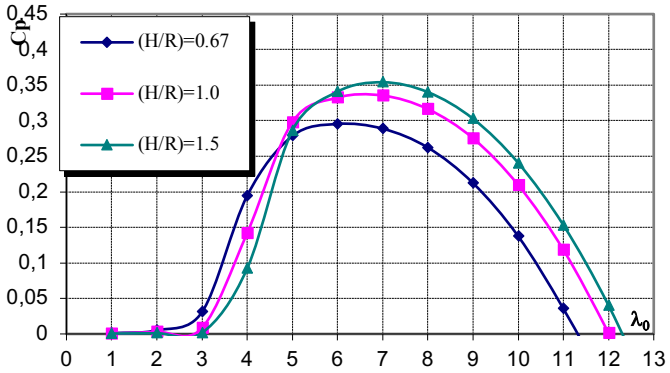

Fig. 10. (H/R) effect on Cp(λ_0) curve for (NC/R) = 0.09.

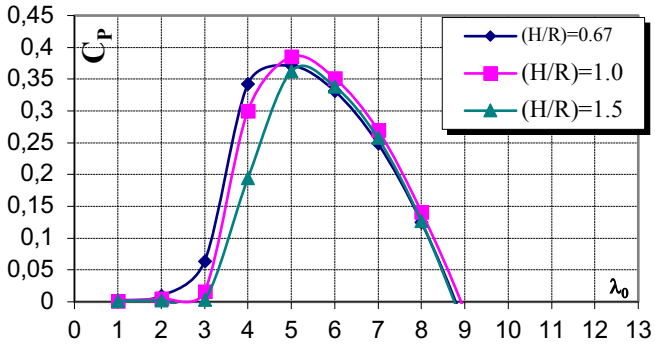

Fig. 11. (H/R) effect on Cp(λ_0) curve for (NC/R) = 0.18.

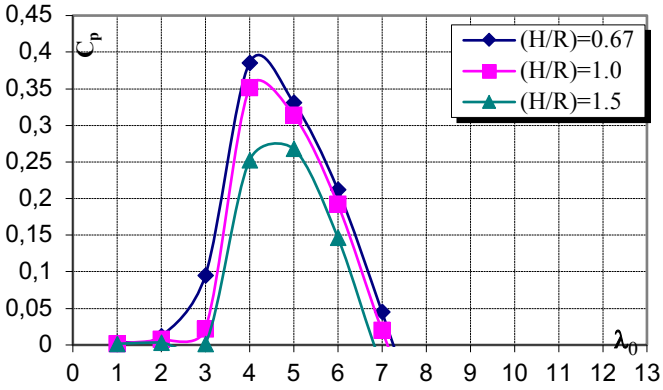

Fig. 12. (H/R) Effect on Cp(λ_0) Curve for (NC/R) = 0.27.

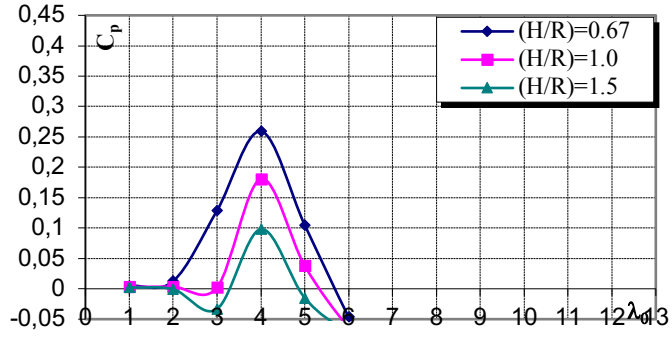

Fig. 13. (H/R) Effect on Cp(λ_0) Curve for (NC/R) = 0.45.

The decrease of Cp with increasing (H/R) over the low λ_0-range in all the four (NC/R) cases may be explained as follows. The increase in the values of (H/R) increases the values of the blade angle "β" in the upper and lower directions of the rotor. This increase in "β" leads in turn to an increase in angel of attack "α" as can be seen in equation **(5).** Now since "α" is excessively high at low values of λ_0 (as in figure 14) the foregoing increase in "α" would undoubtedly leads to a decrease in (C_l/C_d) due to excessive blade flow separation which results in a decrease in Cp. On the other hand, α is typically small over the high λ_0-range so the increase in (H/R) leads to an increase in β which makes the α values rise. This partially contributes to the increase in Cp with increasing (H/R) over the high λ_0-range.

$$\alpha = tan^{-1}\left[\frac{(V/V_1)\sin\theta.\sin\beta}{(V/V_1)\cos\theta+\lambda_0(r/R)}\right] \quad (5)$$

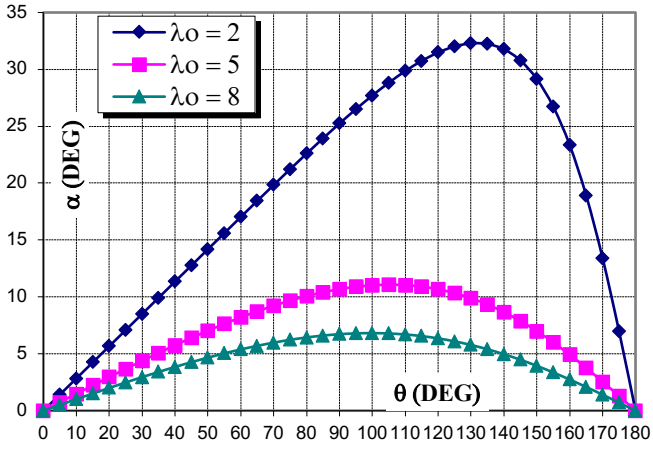

Fig. 14. The contrast α with (θ) for several values of λ_0.

5. Conclusion

In this study, compared to the results of the previous air tunnel test, it turns out that the Multi Stream method, which was represented by a computer program, is able to predict the overall performance of the rotor very well. The results indicated that if the value of (H/R) is constant, it is preferable to deal with the value of (NC/R) instead of dealing with (N) and (C/R) separately. Otherwise, with respect to practical experiments, if the value of (NC/R) is constant, changes in the relative coefficients of N or (C/R) lead to relatively different influences. Moreover, the results of this work clarified that a raise in the value of (NC/R) results in a raise in C_{PM} at first and then decline after that, whilst, the rate of λ_0 which compatible with C_{PM} decreases continuously. In addition, the Cp(λ_0) curves change to take the peak shape more and more, and this reduces the amount of energy extracted in a specific wind speed pattern. Cp increases over low λ_0-range except for (NC/R) values greater than 0.36, while it decreases over very high λ_0-range. Increasing rotor height to diameter ratio leads to a decrease in Cp over low λ_0-range for all values of (NC/R) investigated. However higher values of (H/R) result in an increase in Cp over high λ_0-range for values of (NC/R) less

than 0.2 approximately. Thus, it seems that higher (H/R) values constitute an advantage for fast rotating rotors (low (NC/R) and high λ_0).

References

[1] D.Y. Leung, Y. Yang, Wind energy development and its environmental impact: A review, Renewable and Sustainable Energy Reviews, 16(1) (2012) 1031-1039

[2] P. Mahale, N. Jangid, A. Gite, T.D. Patil, Vertical axis wind turbine: A lucid solution for global small scale energy crisis, Journal of Academia and Industrial Research (JAIR), 3(8) (2015) 393.

[3] A. Tummala, R.K. Velamati, D.K. Sinha, V. Indraja, V.H. Krishna, A review on small scale wind turbines, Renewable and Sustainable Energy Reviews, 56 (2016) 1351-1371.

[4] A. Shires, Design optimisation of an offshore vertical axis wind turbine, Proceedings of the ICE-Energy, 166(EN1) (2013) 7-18.

[5] A. Rezaeiha, H. Montazeri, B. Blocken, Characterization of aerodynamic performance of vertical axis wind turbines: Impact of operational parameters, Energy Conversion and Management, 169 (2018) 45-77.

[6] M. Ghasemian, Z.N. Ashrafi, A. Sedaghat, A review on computational fluid dynamic simulation techniques for Darrieus vertical axis wind turbines, Energy Conversion and Management, 149 (2017) 87-100.

[7] R. Howell, N. Qin, J. Edwards, N. Durrani, Wind tunnel and numerical study of a small vertical axis wind turbine, Renewable energy, 35(2) (2010) 412-422.

[8] J. F. Manwell, J. G. McGowan and A. L. Rogers, "Wind Energy Explained Theory Design and Application," John Wiley & Sons, Hoboken, 2002.

[9] Yan Li. Straight-Bladed Vertical Axis Wind Turbines: History, Performance, and Applications. DOI: 10.5772/intechopen.8476. March 2019.

[10] Doma Hilewit, Edgar Matida, Amin Fereidooni, Hamza Abo el Ella, Fred Nitzsche. "Numerical investigations of a novel vertical axis wind turbine using Blade Element Theory-Vortex Filament Method (BET-VFM)". https://doi.org/10.1002/ese3.438, September 2019.

[11] Doma Hilewit, Edgar Matida, Amin Fereidooni, Hamza Abo el Ella, Fred Nitzsche. "Power coefficient measurements of a novel vertical axis wind turbine" https://doi.org/10.1002/ese3.412. Novmber 2019.

[12] Qian Cheng , Xiaolan Liu , Ho Seong Ji , Kyung Chun Kim and Bo Yang, "Aerodynamic Analysis of a Helical Vertical Axis Wind Turbine", Energies **2017**, 10, 575; 10.3390/en10040575.

[13] Mikhail Ramos, Daniel Sauceda C. "Cfd Study of a Vertical Axis Counter Rotating Wind Turbine" *International Conference on Renewable Energy Research and Applications (ICRERA)*, California, (2017).

[14] Vishal Digambar Bodkhe, "Design and Development of Vortex Blade less Wind Turbine", IJTSRD, www.ijtsrd.com, Volume – 2, Issue – 3, Apr (2018).

[15] Templin R. J. "Aerodynamic Performance Theory for the NRC Vertical -axis Wind Turbine" NRC Lab. Report LTR-LA -190 (June 1974).

[16] Wilson R.E., Lissaman P.B.S. "Applied Aerodynamic of Wind Power Machines" Oregon State University (May 1974).

[17] Strickland J.H. A performance Prediction Model for the Darrieus Turbine" International Symposium on Wind Energy Systems, Cambridge, UK (Sept 1976).

[18] Read S., Sharpe D.J. "An Extended Multiple Streamtube Theory for Vertical-Axis Wind Turbines". 2nd BWEA Workshop, Cranfield, UK (Apr 1980).

[19] Lapin E. E, "Theoretical Performance of Vertical – Axis Wind Turbines", ASME paper, The Winter Annual ASME Meeting Houston, Tx, USA (1975).

[20] Paraschivoiu I. "Double- Multiple Streamtube Model for Darrieus Wind Turbines" 2nd DOE/NASA Wind Turbine Dynamics Workshop, NASA CP 2186, Cleveland, OH, USA (Feb 1981).

[21] Fanucci J.B., Walter R.E. "Innovative Wind Machines: The Theoretical Performance of a Vertical –Axis Wind Turbine". Proceeding of the Vertical-Axis Wind Turbine Technology Workshop. Sandia Laboratories, SAND 76-5586, USA (1976).7

[22] Holame O.A. "Contribution to the Aerodynamic theory of the Vertical-Axis Wind Turbine". International Symposium on Wind Energy Systems. Cambridge, England (sept. 1979).

[23] Strickland J.H., Webster B.T., Nguyen T. "A Vortex Model of the Darrieus Turbine: An Analytical and Experimental Study" J. Fluids Eng., 101 (1979).

[24] Hirsch H., Mandal A. C. "A Cascade Theory for the Aerodynamic Performance of Darrieus Wind Turbines". Wind Engineering, 11(3), (1987).

[25] J.H Strickland , "The Darrieus turbine:A performance prediction model using multiple streamtubes", Sandia Laboratories report no. SAND75-0431, 1975.

[26] Unnikrishan Divakaran, Ratna Kishore Velamati, Ajith Ramesh. "Effect of wind speed on the performance of Troposkein Vertical axis wind turbine". *IJRER*. www.ijrer.org . Vol 8, No 3 (2018).

[27] R.J. de Andrade Vieira and M. A. Sanz-Bobi, "Power curve modelling of a wind turbine for monitoring its behaviour", 2015 *International Conference on Renewable Energy Research and Applications (ICRERA)*, Palermo, doi: 10.1109/ICRERA.2015.7418571. (2015)

[28] Alejandro J. Vitale, Sibila A. Genchi , Andrea P. Rossi , Eduardo D. Guillermo, Horacio R. di Prátula. "Aerodynamic Performance of Straight-Bladed Vertical Axis Wind Turbines: A Practical Open Source Implementation". *International Conference on Renewable Energy Research and Applications (ICRERA)*,Paris, (2018).